Experimental Procedures

Culture Media and Antibodies

The endothelial cell (EC) growth medium (ECGM) contained EBM-2 medium (Cambrex, Walkersville, MD, USA) supplemented with 20% fetal bovine serum (FBS) (Highclone, Logan, UT, USA), EGM-2 MV (Cambrex), 100 U/ml penicillin (Sigma, St. Louis, MO, USA), 100 μl/ml streptomycin (Sigma), and 25 ng/ml amphotericin B (Invitrogen, Grand Island, NY, USA). Control medium (CM) contained Dulbecco's modified Eagle's medium (DMEM; Sigma) supplemented with 10% fetal bovine serum (Highclone), 100 U/ml penicillin (Sigma), 100 μl/ml streptomycin (Sigma), and 25 ng/ml amphotericin B (Invitrogen). Polyclonal anti-claudin-5 and anti-occludin antibodies were purchased from Zymed (San Francisco, CA, USA). The polyclonal anti-hGR antibody was purchased from Santa Cruz (Santa Cruz, CA, USA).

Isolation of Human Peripheral Nerve Microvascular Endothelial Cells Forming the BNB

The study protocol for human peripheral nerve tissue was approved by the ethics committee of the Medical Faculty, Yamaguchi University, and was conducted in agreement with the Declaration of Helsinki, as amended in Somerset West in 1996. Written informed consent was obtained from the patient's family before the tissue was used for the study. Tissue samples were obtained from an adult female who died of an arrhythmia. PnMECs were isolated in accordance with a previously described procedure [14]. Briefly, the sciatic nerve was removed from the patient. The epi- and perineuria were carefully stripped off with fine forceps, mimicking the teased fiber preparation for peripheral nerve pathology. Next, the endoneurium was finely minced with a razor blade and then was digested with 0.25% collagenase type I (Sigma) in 1× Hanks' balanced salt solution (HBSS) (Invitrogen) at 37°C for 2 h in a shaking water bath. After centrifugation (800 g, 5 min), the pellet was suspended in 15% dextran solution, followed by centrifugation for 10 min at 4°C and 5,000 g. The pellet was washed and incubated in a type I collagen-coated dish (Iwaki, Chiba, Japan) at 37°C in a humidified atmosphere of 5% CO_2 and 95% air.

Immortalization and Purification of PnMECs

At 4 days from the first dissemination, cells were incubated overnight with pDON-AI/tsA58, a retroviral vector encoding the open reading frame of the temperature-sensitive SV40 large T antigen. Twelve hours after the beginning of the incubation, cells were washed with HBSS and were subsequently grown at 33°C. This was followed by another overnight incubation with pDON-AI/hTERT, a retroviral vector encoding the open reading frame of hTERT. After the incubation, cells were washed with HBSS and cultured again at 33°C. After endothelial cells (ECs) proliferated sufficiently for cloning, they were picked up with a cloning cup. As ECs grew, non-ECs such as pericytes, fibroblasts, and Schwann cells also appeared and gradually began to occupy the culture area of the dish. These non-ECs were scratched and removed mechanically with a sterilized pointed rubber spatula. After several passages (4 in total) for cloning, one clonal population that consisted of pure endothelial cells, designated "DH-BNBs" was obtained. These DH-BNBs stably grew at the permissive temperature of 33°C. To label them with 1,1'-dioctacecyl-3,3,3',3', tetramethyl indocarbocyanine perchlorate acetylated low-density lipoprotein (DiI-Ac-LDL; Biogenesis, Poole, England), the cells were incubated with 10 μg/ml DiI-Ac-LDL at 33°C in the culture medium overnight. The cells were subsequently viewed under a fluorescence microscope (Olympus, Tokyo, Japan). DH-BNBs incorporated bright DiI-Ac-LDL particles into their cytoplasm.

Quantitative Real-Time PCR Analysis

Total RNA was prepared from PBS-washed cells using an RNeasy® Plus Mini kit (Qiagen, Hilden, Germany). RT and PCR amplification were carried out with TAKARA PCR Thermal Cycler Dice (TakaRa, Otsu, Japan). Single-stranded cDNA was synthesized from 50 ng of total RNA using the StrataScript® First Strand Synthesis System (STRATAGENE®, Cedar Greek, TX, USA) with an oligo-dT primer. A quantitative real-time PCR analysis was performed using a Stratagene Mx3005P (STRATAGENE®, Cedar Greek, TX, USA) with FullVelocity-SYBRGreen QPCR master mix (STRATAGENE®, Cedar Greek, TX, USA) according to the manufacturer's protocol. The sequences of the primers were as follows: claudin-5 forward (ctg ttt cca tag gca gag cg), claudin-5 reverse (aag cag att ctt agc ctt cc), occludin forward (acc ccc atc tga cta tgt gga a), occludin reverse (agg aac cgg cgt gga ttt a), Glyceraldehyde-3-phosphate dehydrogenase (G3PDH) forward (tga agg tcg gag tca acg gat ttg gt), G3PDH reverse (cat gtg ggc cat gag gtc cac cac). G3PDH was used as an internal standard. The samples were subjected to PCR analysis using the following cycling parameters: 95°C for 10 min, 95°C for 15 s and 60°C for 1 min for 40 cycles. Negative controls (cDNA-free solutions) were included in each reaction. The standard reaction curve was analyzed using the MxPro™ (STRATAGENE®, Cedar Greek, TX, USA) software package, and the relative quantity of each

molecule was calculated according to the standard reaction curve.

Western Blot Analysis

DH-BNBs were homogenized in cell lysis buffer containing 10 mM Tris–HCl, pH 7.4, 1 mM EDTA, 0.1% sodium deoxycholate, 1% Triton-X and a protease inhibitor cocktail tablet (Roche). Homogenized samples were centrifuged at 5,000 g for 10 min at 4°C, and the supernatant was subjected to electrophoresis. Twenty micrograms aliquots of protein were fractionated in a 10% gel and electophoretically transferred onto polyvinylidene difluoride membranes. The membrane was blocked at room temperature for 2 h with 5% powdered skimmed milk in PBS containing 0.05% Tween 20 (PBS-T). After that, the membrane was incubated with a primary antibody in PBS-T and 5% milk (1:50) at room temperature for 2 h, followed by incubation with a secondary antibody in PBS-T and 5% milk (1:1,000) at room temperature for 1 h. Membranes were extensively washed in PBS-T and visualized by enhanced chemiluminescence detection (ECL-plus, Amersham, UK). A Densitometric analysis was performed using the Quantity One software program (BIO-RAD, Hercules, CA).

Transendothelial Electrical Resistance Study

The transwell inserts (pore size, 0.4 μm; effective growth area, 0.3 cm^2; BD Bioscience, NJ, USA) were coated with rat tail collagen type-I (BD Bioscience) in accordance with the manufacturer's instructions. DH-BNBs were seeded at 1.0×10^6 cells/insert on the collagen-coated culture inserts at 33°C. After allowing the cells to attach to the bottom of the insert (24–48 h) and become confluent, the TEER of cell layers was measured with a Millicell electrical resistance apparatus (Endohm-6 and EVOM, World Precision Instruments, Sarasota, FL, USA). After becoming confluent, ECGM was removed and cells were cultured in CM with or without 200nM HC. Two days after the medium change, the TEER value was measured. Statistical significance was evaluated using Student's *t* test.

Statistical Analysis

Results are expressed as the means ± SD, and significant differences between groups were determined by Student's *t* test. $P < 0.05$ was considered significant.

Results

Establishment of DH-BNBs

We successfully established a conditionally-immortalized human peripheral nerve microvascular endothelial cell line, "DH-BNB", which was obtained by transfection with retroviruses encoding tsA58 and hTERT. DH-BNBs appear to be closely packed and have a spindle-fiber shaped morphology, which has been thought to characterize endothelial cells constituting barrier systems [4] (Fig. 1A). All (100%) of these cells were positive for Dil-Ac-LDL, thus indicating an excellent purity (Fig. 1B).

DH-BNBs Express the Glucocorticoid Receptor Which can be Significantly Down-Regulated by its Ligand, Hydrocortisone

In order to investigate the sensitivity of DH-BNBs to GCs, we examined GC receptor (GR) expression in this cell line using a Western blot (WB) analysis. In cell lysates from untreated DH-BNBs, there was a strong signal for GR protein detectable by the WB (Fig. 2A). Supplementation with 200nM HC for 48 h led to a prominent reduction in

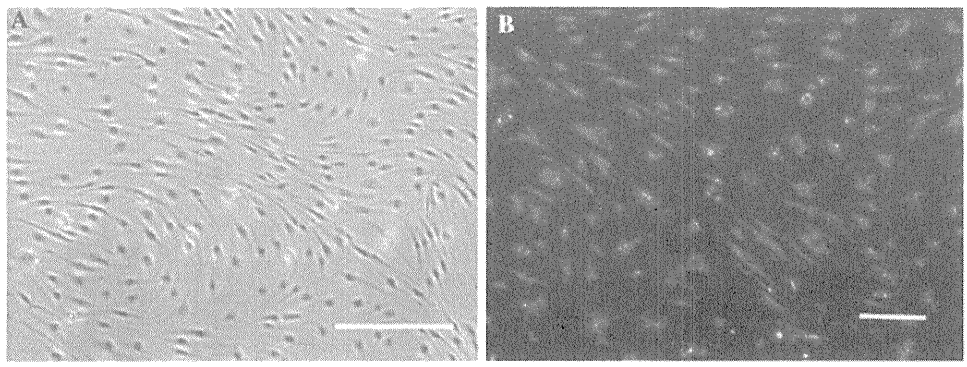

Fig. 1 **a** A phase microscopy image of DH-BNBs. DH-BNBs have a spindle fiber-shaped morphology. **b** All of the cells were positive for Dil-Ac-LDL. *Scale bar* 100 μm

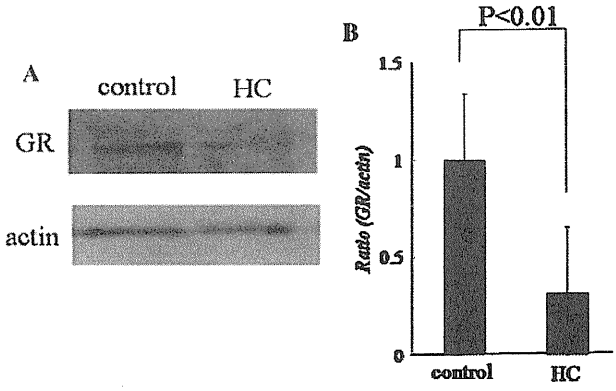

Fig. 2 GR protein expression in the DH-BNBs. After reaching confluence in ECGM, DH-BNBs were incubated in CM with or without 200nM HC. After 48 h of incubation, cell lysates were analyzed by WB for GR protein (**a**).HC supplementation led to a reduction in detectable GR protein to 31.4 ± 6.0% of the control cells as determined by a densitometric analysis of the WB results (**b**)

GR protein to 31.4 ± 6.0% the level of untreated cells, as evaluated by densitometric analysis of the WB data (Fig. 2B).

The mRNA Expression of Tight Junction Molecules in Response to HC Treatment in DH-BNBs

To assess the effects of GCs on tight junction molecules, DH-BNBs were grown in culture to confluence and treated with 200nM HC. After 48 h of HC treatment, total RNA was isolated from the DH-BNBs and was processed for RT–PCR analysis. Although the expression level of occludin in the DH-BNBs was unchanged, that of claudin-5 significantly increased by HC treatment (Fig 3A, B).

HC Treatment Increases the Content of the Tight Junction Protein, claudin-5

To examine the effects of GCs on the tight junction protein content in the BNB, DH-BNBs were grown to confluence and incubated in CM with or without HC. After 48 h, cell lysates were analyzed by a WB analysis using polyclonal antibodies for claudin-5 and occludin. We observed a significant increase in the claudin-5 protein content (Fig. 4A). On the other hand, the expression of occludin protein was unchanged by HC application (Fig. 4B).

Hydrocortisone Enhances the Barrier Properties of DH-BNBs

To further validate whether GCs could enhance the barrier properties of DH-BNBs, we measured the TEER across the DH-BNB monolayer incubated in CM with or without HC. HC supplementation led to a significant increase in the TEER across the DH-BNB monolayer, indicating that HC enhanced the barrier properties of DH-BNBs (Fig 5).

Discussion

In the BBB, several proteins have been reported to be localized at TJs, including occludin [15] and claudin-5 [16]. Occludin is highly expressed and consistently presents in a distinct, continuous pattern along the cell margins in the cerebral endothelium [17] whereas it is much more sparsely distributed in non-neural endothelial cells [18]. Claudin-5 is now recognized as the most important protein involved in maintaining the BBB function [16] and was reported to be the most abundantly expressed subtype among claudins in mouse brain capillary endothelial cells at the mRNA level [19]. Ohtsuki et al. also reported that exogenous expression of claudin-5 induces barrier properties in cultured rat brain capillary endothelial cells [20]. These two important TJ proteins were expressed in our human in vitro BNB model. This result is consistent with the results obtained using rat PnMECs, indicating that the endothelium constituting the BNB express the same tight

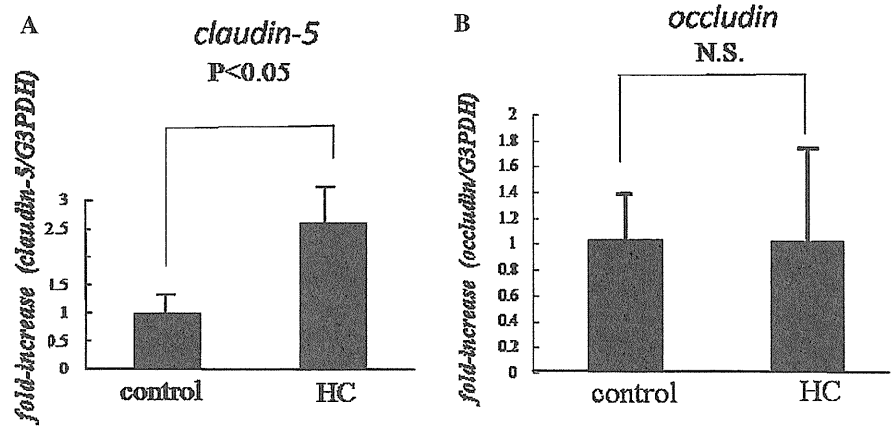

Fig. 3 Effects of HC on the mRNA expression of tight junction molecules. After reaching confluence, DH-BNBs were incubated in CM with or without 200nM HC. After a 48 h-incubation, total RNA was extracted and processed for real-time PCR analysis. HC up-regulated claudin-5 mRNA expression (**a**) (2.68 ± 1.2-fold) but did not increase that of occludin (**b**)

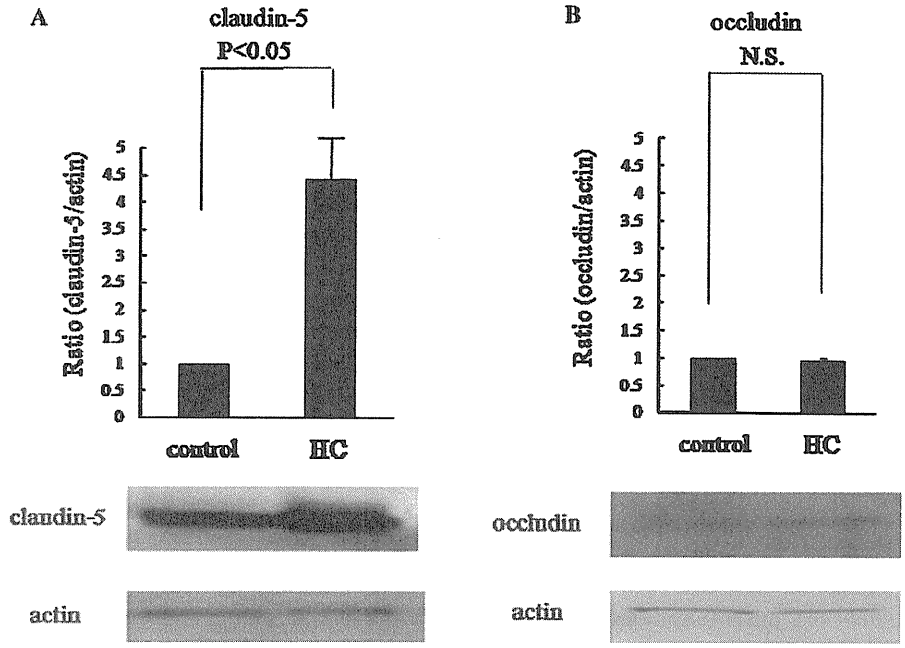

Fig. 4 The effect of HC on two TJ proteins, claudin-5 and occludin, was examined by WB and densitometric analysis. Cells were treated with 200nM HC for 48 h, and subjected to SDS–PAGE and WB. Densitometric evaluation resulted in an 4.45 ± 1.4-fold (n = 3) up-regulation of claudin-5 protein in cells in the presence of HC (**a**), while occludin protein levels remain unchanged (**b**)

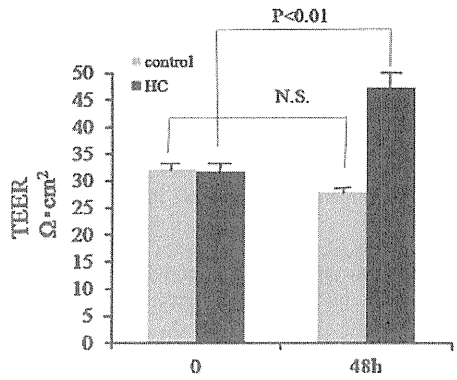

Fig. 5 The influence of HC on TEER values of DH-BNB monolayers was examined. After reaching confluence on cell culture inserts, DH-BNBs were incubated in CM with or without HC. After 48 h of incubation, the TEER was measured. The TEER of cells incubated in CM with HC significantly increased, while that of the control group did not change. *Data* are presented as means ± SD (n = 6)

junction molecules expressed in the BBB, including claudin-5 and occludin [4].

Breakdown of the BNB has been reported in many disorders of the human peripheral nervous system. In sural nerve biopsy specimens, several BNB changes, including fenestration or gaps between adjacent PnMECs and a lack of tight junctions, have been described in some inflammatory neuropathies such as CIDP [5] and macroglobulinemic neuropathy [7, 21, 22]. CIDP is a chronic progressive or relapsing neuropathy and is regarded as an autoimmune disease involving cellular and humoral immunity [23, 24]. Kanda et al. reported that the percentage of claudin-5-positive microvessels in the endoneurium of patients suffering from CIDP was significantly decreased compared with that of patients with non-inflammatory neuropathies [6]. In this article, no appreciable difference in immunoreactivity for occludin was noted between CIDP and the non-inflammatory neuropathy group. These results indicate the possibility that decreased claudin-5 in the PnMECs is responsible for TJ damage, leading to a leaky BNB in patients with CIDP. The loss of claudin-5 and breakdown of TJs in CIDP may enhance the leakage of inflammatory cytokines, as well as, immunoglobulins into the endoneurial space, and may result in changes to the endoneurial constituents that are unfavorable to Schwann cells and axons, eventually leading to a worsening of the neuropathy. Hence, the restoration of the dysfunctional BNB could represent an effective new therapeutic strategy that could be used in combination with immnunosuppression in CIDP patients.

The GCs are a class of steroid hormones that are commonly used to treat acute and chronic inflammatory disorders [25]. They exert most of their functions by binding to the GR, which controls the gene expression and signaling cascades through both genomic and non-genomic mechanisms. Our results indicated that GR protein in DH-BNBs is reduced in the presence of hydrocortisone (Fig 2A, B). Hormone-dependent down-regulation of GR has been demonstrated previously [26]. Notably, it is reported that HCs down-regulated GR and brought the up-regulation of ocludin and claudin-5 at the mRNA and protein levels in immortalized human brain endothelial cells [13]. It is uncertain how the decreased GR in the presence of HC bring the up-regulation of tight junction

molecules. However, the previous report and our results demonstrate that HCs induce the up-regulation of tight junction proteins in spite of the down-regulation of GR in the endothelial cells derived from the BBB and the BNB. Further analyses are needed to elucidate the precise mechanism of the up-regulation of tight junction molecules with reduced expression of GR.

Importantly, GCs have been widely used in the treatment of CIDP [8, 9]. Although the immunosuppresive and anti-inflammatory effects of GCs have been thought to be their major mechanism of action, the effect of GCs on the pathophysiology of CIDP has not been completely clarified. Our results suggest that GCs might increase the BNB function and work partially for clinical improvement through up-regulation of endothelial claudin-5 in CIDP patients.

Several studies using in vitro BBB models have shown that GCs can enhance the barrier properties of the BBB. Förster reported that HC induced an increase of occludin at both the mRNA and protein levels, and enhanced the barrier properties in a murine immortalized brain capillary endothelial cell line [12]. The same group also showed that HC up-regulated claudin-5 and occludin at both the mRNA and protein levels and increased the barrier properties in a human brain microvascular endothelial cell line [13]. We also found significant enhancement of barrier properties and an increase in claudin-5 expression in DH-BNBs after HC application, although there were no changes in the expression of occludin. It is unclear whether these differences may be caused by the different environments between the BBB and BNB, and future studies of the molecular dynamics of TJ proteins using PnMECs derived from human peripheral nerves may improve the understanding of BNB derangement and prompt the development of new therapeutic approaches for these inflammatory neuropathies. Our novel human cell line, DH-BNBs, is therefore expected to help in the performance of such studies and will also be useful for identifying potential therapeutic agents that can increase the BNB function.

Acknowledgments This work was supported in part by a Neuroimmunological Disease Research Committee grant from the Ministry of Health, Labour and Welfare, Japan and also by a Grant-in-Aid for Scientific Research from the Ministry of Education, Science, Sports and Culture, Japan.

References

1. Poduslo JF, Curran GL, Berg CT (1994) Macromolecular permeability across the blood-nerve and blood-brain barriers. Proc Natl Acad Sci USA 91:5705–5709
2. Bell MA, Weddell AGM (1984) A descriptive study of the blood vessels of the sciatic nerve in the rat, man, and other mammals. Brain 107:871–898
3. Latker CH, Wadhwani KC, Balbo A, Rapoport SI (1991) Blood-nerve barrier in the frog during Wallerian degeneration: Are axons necessary for maintenance of barrier functions? J Comp Neurol 309:650–664
4. Sano Y, Shimizu F, Nakayama H et al (2007) Endothelial cells constituting blood-nerve barrier have highly specialized characteristics as barrier-forming cells. Cell Struct Funct 32:139–147
5. Kanda T, Yamawaki M, Iwasaki T et al (2000) Glycosphingolipid antibodies and blood-nerve barrier in autoimmune demyelinative neuropathy. Neurology 54:1459–1464
6. Kanda T, Numata Y, Mizusawa H (2004) Chronic inflammatory demyelinating polyneuropathy: decreased claudin-5 and relocated ZO-1. J Neurol Neurosurg Psychiatry 75:765–769
7. Lach B, Rippstein P, Atack D et al (1993) Immunoelectron microscopic localization of monoclonal IgM antibodies in gammopathy associated with peripheral demyelinative neuropathy. Acta Neuropathol 85:298–307
8. Dyck PJ, O'Brien PC, Oviatt KF et al (1982) Prednisone improves chronic inflammatory demyelinating polyradiculoneuropathy more than no treatment. Ann Neurol 11:136–141
9. Hughes R, Bensa S, Willison H et al (2001) Randomized controlled trial of intravenous immunoglobulin versus oral prednisolone in chronic inflammatory demyelinating polyradiculoneuropathy. Ann Neurol 50:195–201
10. Miller DH, Thompson AJ, Morrissey SP et al (1992) High dose steroids in acute relapses of multiple sclerosis: MRI evidence for a possible mechanism of therapeutic effect. J Neurol Neurosurg Psychiatry 55:450–453
11. Schmidt J, Metselaar JM, Wauben MH et al (2003) Drug targeting by long-circulating liposomal glucocorticosteroids increases therapeutic efficacy in a model of multiple sclerosis. Brain 126:1895–1904
12. Förster C, Silwedel C, Golenhofen N et al (2005) Occludin as direct target for glucocorticoid-induced improvement of blood-brain barrier properties in a murine in vitro system. J Physiol 565:475–486
13. Förster C, Burek M, Romero IA et al (2008) Differential effects of hydrocortisone and TNFalpha on tight junction proteins in an in vitro model of the human blood-brain barrier. J Physiol 586:1937–1949
14. Kanda T, Iwasaki T, Yamawaki M et al (1997) Isolation and culture of bovine endothelial cells of endoneurial origin. J Neurosci Res 49:769–777
15. Furuse M, Hirase T, Itoh M et al (1993) Occludin: A novel integral membrane protein localizing at tight junctions. J Cell Biol 123:1777–1788
16. Nitta T, Hata M, Gotoh S et al (2003) Size-selective loosening of the blood-brain barrier in claudin-5-deficient mice. J Cell Biol 161:653–660
17. Hawkins BT, Davis TP (2005) The blood-brain barrier/neurovascular unit in health and disease. Phamacol Rev 57:173–185
18. Hirase T, Staddon JM, Saitou M (1997) Occludin as a possible determinant of tight junction permeability in endothelial cells. J Cell Sci 110:1603–1613
19. Ohtsuki S, Yamaguchi H, Katsukura Y et al (2008) mRNA expression levels of tight junction protein genes in mouse brain capillary endothelial cells highly purified by magnetic cell sorting. J Neurochem 104:147–154
20. Ohtsuki S, Sato S, Yamaguchi H et al (2007) Exogenous expression of claudin-5 induces barrier properties in cultured rat brain capillary endothelial cells. J Cell Physiol 210:81–86
21. Kanda T, Usui S, Beppu H et al (1998) Blood-nerve barrier in IgM paraproteinemic neuropathy: a clinicopathologic assessment. Acta Neuropathol 95:184–192
22. Meier C, Roberts K, Steck A et al (1984) Polyneuropathy in Waldenström's macroglobulinaemia: reduction of endoneurial

IgM-deposits after treatment with chlorambucil and plasmapheresis. Acta Neuropathol 64:297–307
23. Köller H, Kieseier BC, Jander S et al (2005) Chronic inflammatory demyelinating polyneuropathy. N Engl J Med 352:1343–1356
24. Vallat JM, Sommer C, Magy L (2010) Chronic inflammatory demyelinating polyradiculoneuropathy: diagnostic and therapeutic challenges for a treatable condition. Lancet Neurol 9:402–412
25. Tuckermann JP, Kleiman A, McPherson KG et al (2005) Molecular mechanisms of glucocorticoids in the control of inflammation and lymphocyte apoptosis. Crit Rev Clin Lab Sci 42:71–104
26. Heitzer MD, Wolf IM, Sanchez ER et al (2007) Glucocorticoid receptor physiology. Rev Endocr Metab Disord 8:321–330

A Case of Systemic Sclerosis with Sarcoidosis

Hiraku Suga[1], Yoshihide Asano[1]*, Zenshiro Tamaki[1], Mizuho Yamamoto[1], Makoto Sugaya[1], Jun Shimizu[2] and Shinichi Sato[1]
*[1]Department of Dermatology, Faculty of Medicine, University of Tokyo, 7-3-1 Hongo, Bunkyo-ku, Tokyo 113-8655, and [2]Department of Neurology, Graduate School of Medicine, University of Tokyo, Tokyo, Japan. *E-mail: yasano-tky@umin.ac.jp*
Accepted March 16, 2011.

Sarcoidosis is a Th1-mediated multisystem granulomatous disorder characterized by lymphadenopathy, internal organ involvement, and a variety of skin lesions. Systemic sclerosis (SSc) is a multisystem autoimmune disorder characterized by vascular injuries and fibrosis of the skin and various internal organs. Th2 polarized immune responses have been shown in the early and active stage of SSc (1). We report here a case of rare overlap of SSc with sarcoidosis, occurring in a female patient with lupus pernio, sarcoid myopathy and interstitial lung disease (ILD).

CASE REPORT

A 59-year-old woman was referred to our hospital for further examination of sclerodactyly and muscle weakness. One year previously, Raynaud's phenomenon had developed on all fingers of both hands. Two months prior to presentation, sclerodactyly had developed. Muscle weakness was also seen. The patient's medical history revealed a radical operation for colon cancer when she was 52 years old. No cytotoxic drugs were administered after the surgery.

Physical examination revealed sclerosis and swelling of all fingers (Fig. 1a) and a shiny, up to egg-sized, sclerotic plaque on the right buttock (Fig. 1b). The patient also had indurated chilblain-like erythema on the palms (Fig. 1c). Raynaud's phenomenon and nailfold bleeding were seen. The strength of bilateral deltoid and triceps muscles was grade 4 (normal: 5) on manual muscle testing. Laboratory tests revealed positive serum anti-nuclear antibody (×320, speckled) and an elevated serum anti-U1 RNP antibody level of 131.1 Index (normal 0–21 Index). Anti-Sm, anti-topoisomerase I, anti-centromere, and anti-Jo-1 antibodies were all negative. The patient had an elevated level of C-reactive protein (CRP) 1.11 mg/dl (0–0.3 mg/dl), elevated creatinine phosphokinase (CK) 300 IU/l (0–50 IU/l), elevated aldolase 9.8 U/l (2.5–6.2 U/l), and elevated KL-6 571 U/ml (0–500 U/ml). Serum surfactant protein-D and calcium levels, and liver and kidney functions were all within normal ranges. Pulmonary function tests revealed that the percentage of predicted vital capacity was 92%, forced expiratory volume1.0/ forced vital capacity 83%, and the percentage of predicted diffusing lung capacity for carbon monoxide 80%.

A skin biopsy was taken from the buttock sclerosis. Histopathology revealed thickened collagen bundles throughout the reticular dermis, especially in the deep dermis (Fig. 2a). According to the classification criteria proposed by LeRoy et al. (2), we diagnosed the patient with limited cutaneous SSc. Due to the clinical features of muscle weakness and elevated muscle enzymes, we suspected that she also had polymyositis. Magnetic resonance imaging showed inflammation in the left deltoid muscle. Histopathological examination of the left deltoid muscle showed non-caseating granulomas with Langhans' giant cells between muscle fibres (Fig. 2b and c). Lymphocytic infiltration and slight degeneration of muscle fibres were also seen, but not to a degree that could be labelled polymyositis. Based on these findings, we diagnosed her muscle involvement as sarcoid myopathy. Serum

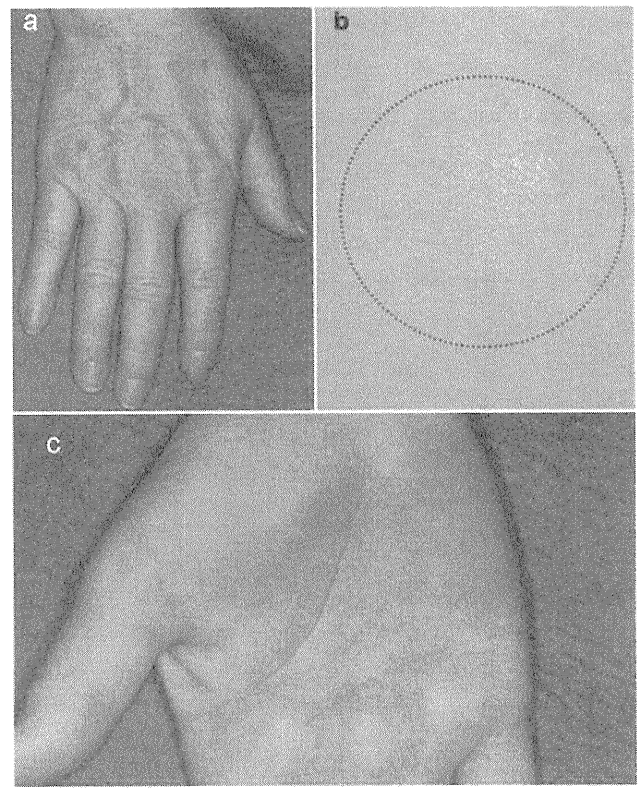

Fig. 1. (a) Sclerosis and swelling of all fingers. (b) A shiny and up to egg-sized sclerotic plaque on the right buttock. (c) Indurated chilblain-like erythema on the palm.

lysozyme was elevated to 11.0 μg/ml (normal 5.0–10.2 μg/ml), while angiotensin-converting enzyme was normal. Tuberculin skin test showed negative reaction. Computed tomography of the chest showed mediastinal and bilateral hilar lymphadenopathy, and ground-glass opacity in the basal segment of both lungs. We also took a skin biopsy from the indurated erythema on the right palm. Non-caseating granulomas were seen in the dermis and adipose tissue (Fig. 2d). Extensive studies failed to reveal other organ involvements, including ocular lesions, neurosarcoidosis, and myocardial sarcoidosis. Oral prednisone was started at a dose of 30 mg/day. Serum CK and CRP levels were normalized after 8 days. Skin lesions including buttock sclerosis, ILD, and hilar lymphadenopathy also responded to the treatment. Prednisone was tapered gradually to 17.5 mg/day with no relapse of sarcoidosis-associated symptoms during the 9-month follow-up period.

DISCUSSION

To our knowledge, 21 overlap cases of sarcoidosis with SSc have been reported in the English literature

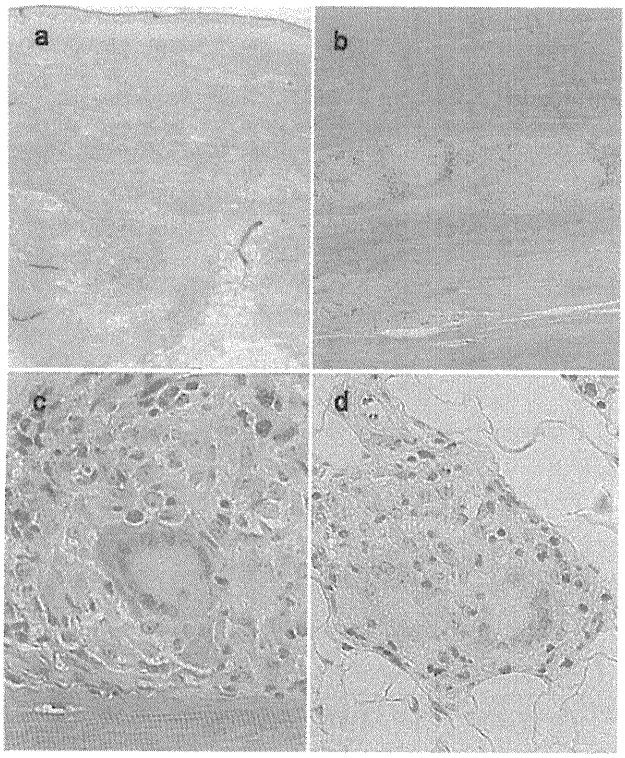

Fig. 2. (a) In the right buttock sclerosis, collagen fibres were increased and swollen throughout the reticular dermis, especially in the deep dermis (haematoxylin-eosin stain, original magnification ×40). (b) Non-caseating granulomas between muscle fibres, slight lymphocytes infiltration, and degeneration of muscle fibres were seen (×100). (c) Langhans' giant cells were seen (×400). (d) Non-caseating granulomas with Langhans' granuloma cells were also seen in the palmar chilblain-like erythema (×400).

(3–11). The incidence of the overlap cases appears to be lower than expected, given the incidence of sarcoidosis (50–400/million/year) and the incidence of SSc (20/million/year) (12, 13). The Th1/Th2 paradigm provides one possible explanation for this. For example, sarcoidosis has been reported to be associated with a low incidence of atopy and allergic diseases characterized by Th2 immune responses (14). On the other hand, atopy improves the disease activities and the clinical courses of several Th1-mediated diseases, such as rheumatoid arthritis, multiple sclerosis, and sarcoidosis (15). Given that Th2 immune responses are predominant in the early and/or active stage of SSc (1), the overlap of Th1-mediated sarcoidosis with early and/or active SSc should theoretically be rare.

When assessing the clinical relevance of SSc with sarcoidosis, it is important to focus on the cases in which SSc precedes sarcoidosis, or in which the two diseases develop simultaneously, because sarcoidosis may be self-limiting. Therefore, we scrutinized the previously reported 9 cases meeting this criterion (3, 4). Although ILD existed in most of the cases, exacerbation of ILD that was probably due to sarcoidosis was not reported. Given that ILD is progressive and life-threatening in a certain subset of sarcoidosis, these previous observations suggest that the clinical course of sarcoidosis associated with SSc is milder than others, supporting the conventional Th1/Th2 paradigm, as described above. Importantly, this was also the case in our patient. She developed SSc and sarcoidosis simultaneously and she had ILD and myopathy associated with sarcoidosis. However, both of these involvements were mild, and fairly responsive to corticosteroid. Thus, the co-existence of SSc with sarcoidosis may serve as a useful clinical clue to predict a milder disease course of sarcoidosis.

Sarcoidosis in SSc is probably often misdiagnosed because organ involvements in sarcoidosis are quite similar to those of many other collagen diseases. Lupus pernio is clinically similar to chilblain erythema and can be misdiagnosed in association with impaired peripheral circulation, such as SSc. ILD frequently occurs in both sarcoidosis and SSc. Furthermore, myositis occasionally coexists with SSc, and it is indistinguishable from sarcoid myopathy without muscle biopsy, especially in cases in which muscle weakness is prominent in the proximal extremity muscle groups. Biopsy of the skin and/or muscle may be useful to determine the origin of ILD in cases with overlapping SSc and sarcoidosis.

REFERENCES

1. Matsushita T, Hasegawa M, Hamaguchi Y, Takehara K, Sato S. Longitudinal analysis of serum cytokine concentrations in systemic sclerosis: association of interleukin 12 elevation with spontaneous regression of skin sclerosis. J Rheumatol 2006; 33: 275–284.
2. LeRoy EC, Black C, Fleischmajer R, Jablonska S, Krieg T, Medsger TA Jr, et al. Scleroderma (systemic sclerosis): classification, subsets and athogenesis. J Rheumatol 1988; 15: 202–205.
3. De Bandt M, Perrot S, Masson CH, Meyer O. Systemic sclerosis and sarcoidosis, a report of five cases. Br J Rheumatol 1997; 36: 117–119.
4. Sakamoto N, Ishimimatsu Y, Kakugawa T, Hara A, Hara S, Amenomori M, et al. Sarcoidosis in a patient with systemic sclerosis and primary biliary cirrhosis. Intern Med 2010; 49: 1609–1611.
5. Borges da Costa J, Mayer-da-Silva A, Soares de Almeida LM, Marques Gomes M. Success of prednisone in the treatment of a patient with sarcoidosis and systemic sclerosis: report of a case. Dermatol Online J 2009; 102: 11.
6. Groen H, Postma DS, Kallenberg CGM. Interstitial lung disease and myositis in a patient with simultaneously occurring sarcoidosis and scleroderma. Chest 1993; 104: 1298–1300.
7. Cox D, Conant E, Earle L, Newman J, Kahalah B, Jimenez S, et al. Sarcoidosis in systemic sclerosis: report of 7 cases. J Rheumatol 1995; 22: 881–885.
8. Wiesenhuther C, Sharma O. Is sarcoidosis an autoimmune disease? Report of four cases and review of the literature. Arthritis Rheum 1979; 9: 124–144.
9. Maekawa Y, Nogami R. A case of progressive systemic sclerosis associated with sarcoidosis and esophageal adenocarcinoma. J Dermatol 1993; 20: 45–48.
10. Sharma O, Ahamad I. The CREST syndrome and sarcoidosis. Another example of overlap syndrome. Sarcoidosis

1988; 5: 71–73.
11. Enzenauer RJ, Xest SG. Sarcoidosis in autoimmune diseases. Semin Arthritis Rheum 1992; 22: 1–17.
12. Lazarus A. Sarcoidosis: epidemiology, etiology, pathogenesis, and genetics. Dis Mon 2009; 55: 649–660.
13. Mayes MD, Lacey JV Jr, Beebe-Dimmer J, Gillespie BW, Cooper B, Laing TJ, Schottenfeld D. Prevalence, incidence, survival, and disease characteristics of systemic sclerosis in a large US population. Arthiritis Rheum 2003; 48: 2246–2255.
14. Kokturk N, Han ER, Turktas H. Atopic status in patients with sarcoidosis. Allergy Asthma Proc 2005; 26: 121–124.
15. Romagnani S. T-cell subsets (Th1 versus Th2). Ann Allergy Asthma Immunol 2000; 85: 9–18.

Neurogenetics (2011) 12:259–261
DOI 10.1007/s10048-011-0284-7

LETTER TO THE EDITORS

Adult-onset leukoencephalopathies with vanishing white matter with novel missense mutations in *EIF2B2*, *EIF2B3*, and *EIF2B5*

Takashi Matsukawa · Xuemin Wang · Rui Liu · Noel C. Wortham · Yuko Onuki · Akatsuki Kubota · Ayumi Hida · Hisatomo Kowa · Yoko Fukuda · Hiroyuki Ishiura · Jun Mitsui · Yuji Takahashi · Shigeki Aoki · Shunya Takizawa · Jun Shimizu · Jun Goto · Christopher G. Proud · Shoji Tsuji

Received: 13 March 2011 / Accepted: 14 March 2011 / Published online: 12 April 2011

Leukoencephalopathy with vanishing white matter (VWM) is a type of leukoencephalopathy with autosomal recessive inheritance. Magnetic resonance imaging (MRI) reveals diffuse leukoencephalopathy with lesions having cerebrospinal fluid (CSF)-like signals. The clinical presentations include progressive cerebellar ataxia, spasticity, and mental decline. The course is chronic progressive with episodes of rapid deterioration following a minor head trauma. Mutations in the five gene-encoding subunits of the translation initiation factor eIF2B, *EIF2B1-5*, have been identified as the causative mutations for VWM. Although the age at onset of VWM is usually 2–6 years, patients with adult onset have been described. All adult-onset cases except one have been found to be associated with mutations in *EIF2B5* [1]. We report cases of adult-onset VWM with novel missense mutations in *EIF2B2*, *EIF2B3*, and *EIF2B5*, which showed decreased eIF2B activities.

Case 1: A Japanese woman aged 56 who experienced secondary amenorrhea and juvenile cataracts during her early 20s. Clumsiness in her hands and gait unsteadiness appeared at age 43. Leg weakness and gait unsteadiness worsened, occasionally in a phased manner after a minor trauma. Forgetfulness appeared at age 54.

Case 2: A Japanese man aged 53 who noticed gait unsteadiness and miscalculation at age 50. Gait unsteadiness worsened, sometimes in a phased manner after a minor trauma.

Case 3: A Japanese woman aged 30 who experienced secondary amenorrhea at age 28. She noticed hemianopia on the left at age 29. She noticed weakness in her left leg after a fall.

All of three cases had parents who were first cousins. MRI of the three cases showed leukoencephalopathy with lesions having CSF-like signals (Supplementary Fig. 1A–I).

The multipoint parametric linkage study (autosomal recessive model) using the 100K SNP array (Affymetrix, Santa Clara, CA, USA) identified homozygous regions in

Electronic supplementary material The online version of this article (doi:10.1007/s10048-011-0284-7) contains supplementary material, which is available to authorized users.

T. Matsukawa · A. Kubota · A. Hida · Y. Fukuda · H. Ishiura · J. Mitsui · Y. Takahashi · J. Shimizu · J. Goto · S. Tsuji (✉)
Department of Neurology, Graduate School of Medicine,
The University of Tokyo,
7-3-1, Hongo, Bunkyo-ku,
Tokyo 113-8655, Japan
e-mail: tsuji@m.u-tokyo.ac.jp

X. Wang · R. Liu · N. C. Wortham · C. G. Proud
School of Biological Sciences, Life Sciences Building,
University of Southampton,
Southampton, UK

Y. Onuki · S. Takizawa
Department of Neurology, Graduate School of Medicine,
University of Tokai,
Kanagawa, Japan

H. Kowa
Department of Neurology, Graduate School of Medicine,
Kobe University,
Hyogo, Japan

S. Aoki
Department of Radiology, Graduate School of Medicine,
University of Juntendo,
Tokyo, Japan

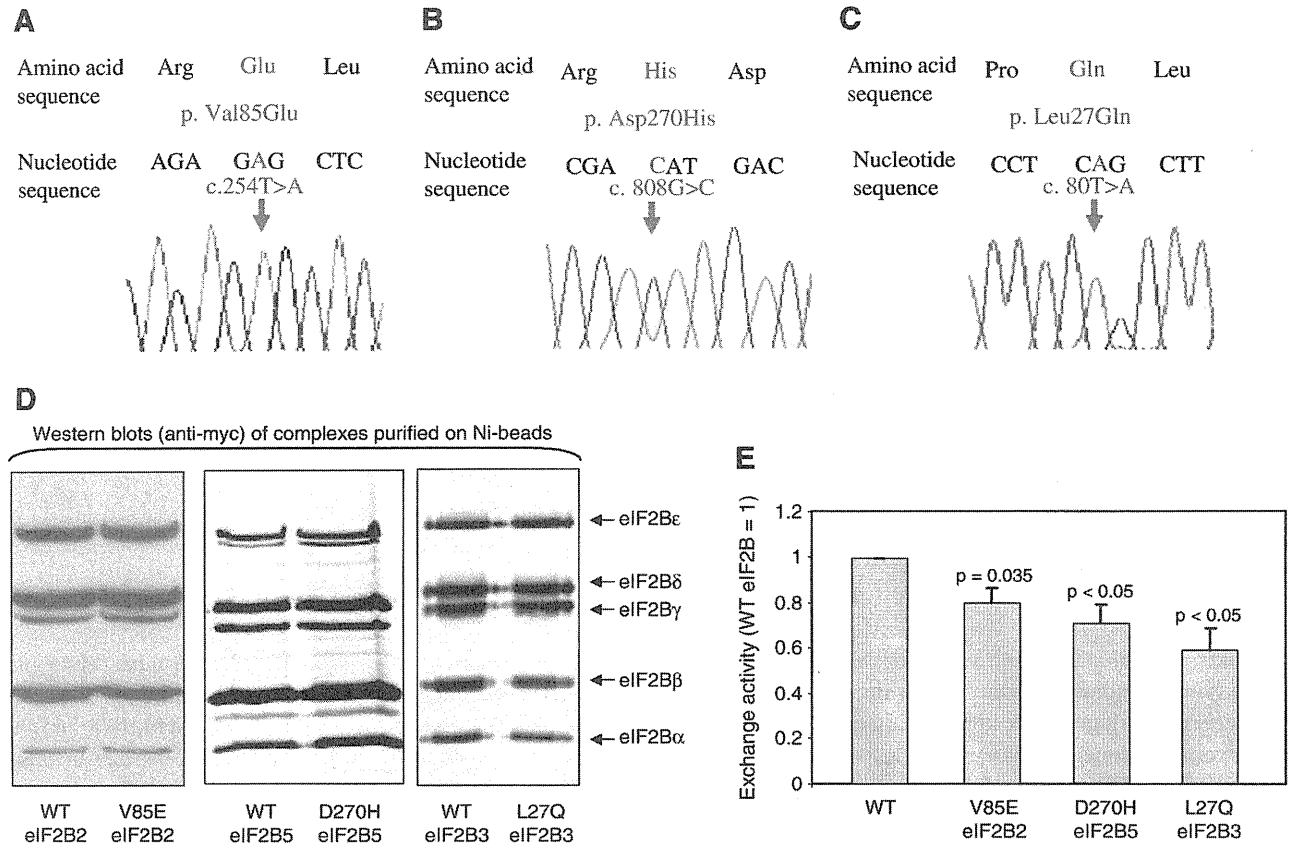

Fig. 1 A homozygous novel (p.Val85Glu) *EIF2B2* was identified (**a**) in case 1. A homozygous novel mutation (p.Asp270His) in *EIF2B5* was identified (**b**) in case 2. A homozygous novel mutation (p.Leu27Gln) in *EIF2B3* was identified (**c**) in case 3. Analyses of formation and activity of eIF2B complexes containing eIF2Bβ[V85E], eIF2Bε[D270H], or eIF2Bγ[L27Q], compared with data on complexes containing the corresponding WT subunits (**d** and **e**). In each case, the other four subunits are also WT. (**d**) Results of Western blotting with anti-myc antibody of eIF2B subunits in complexes isolated by virtue of the His_6-tag on eIF2Bβ, eIF2Bε, or eIF2Bγ, respectively. There are clearly equal amounts of the β, δ, and ε subunits. Although the signals for eIF2Bγ and α are weaker, the signal intensities of the subunits are the same as those of the WT and "mutant" complexes. (**e**) Effects of the mutant eIF2Bβ, eIF2Bε, or eIF2Bγ subunit on activity of eIF2B. There is a decrease of about 20%, 30%, or 40% in the GDP/GTP exchange activity of eIF2B-containing mutant eIF2Bβ (p.Val85Glu), eIF2Bε (p. Asp270His), or eIF2Bγ (p.Leu27Gln), respectively, when compared with eIF2B complexes containing the corresponding WT eIF2B subunits. Each experiment was performed five times, with duplicate or triplicate assays of activity in each case: data are given as % wild-type control±SEM

each of the three cases (case 1; *EIF2B1* and *EIF2B2*, case 2; *EIF2B5*, and case 3; *EIF2B5*) (Supplementary Fig. 2A–C). In accordance with these results, mutational analyses revealed a homozygous mutation (c.375T>A) in *EIF2B2* resulting in the substitution of glutamic acid for valine (p. Val85Glu), a homozygous mutation (c.808 G>C) in *EIF2B5* resulting in the substitution of aspartic acid for histidine (p. Asp270His), and a homozygous mutation (c.80T>A) in *EIF2B3* resulting in the substitution of leucine for glutamine (p.Leu27Gln) in cases 1, 2, and 3, respectively (Fig. 1a–c). No mutations were identified in other subunit genes. These mutations were not described previously and were not present in 96 unrelated Japanese control subjects. Case 3 was the first among cases of adult-onset VWM with the mutation in *EIF2B3*. Case 1 was the second among the adult-onset cases with the mutation in *EIF2B2*.

We then analyzed activities of eIF2B GEF-containing mutant *EIF2B* subunits as previously described [2]. The GDP/GTP exchange activity of eIF2B containing the mutant eIF2Bβ (Val85Glu) subunit decreased by approximately 20% compared with that of eIF2B containing the wild-type (WT) eIF2Bβ subunit (Fig. 1e). Similarly, the GDP/GTP exchange activities of eIF2B containing the mutant eIF2Bγ (Leu27Gln) and eIF2Bε (Asp270His) subunits substantially and significantly decreased compared with that of eIF2B containing WT eIF2Bγ or ε (Fig. 1e). Interestingly, the decrease in the GDP/GTP exchange activity of the eIF2B complexes containing the mutant eIF2Bβ is milder than those previously reported for mutations identified in cases of childhood-onset VWM [2], raising the possibility that mild decreases in eIF2B activity may be associated with later ages at onset. Intriguingly, the residual activity of eIF2B (eIF2B3

[L27Q]) is lower than that of eIF2B (eIF2B2[V85E] or eIF2B5[D270H]), which may be consistent with an earlier age at onset in case 3. Further detailed investigation on a much larger number of cases of VWM will be needed to confirm whether residual activity is related to the age at onset and the variability of the VWM phenotype.

Acknowledgments This work was supported in part by KAKENHI (Grant-in-Aid for Scientific Research) on Priority Areas, Innovative Areas, Global COE Program for Chemical Biology of the Diseases, and Scientific Research (A) from the Ministry of Education, Culture, Sports, Science and Technology of Japan, and a Grant-in-Aid for Research on Intractable Diseases and Comprehensive Research on Disability Health and Welfare from the Ministry of Health, Welfare and Labour, Japan. CGP gratefully acknowledges the support from the UK Biotechnology and Biotechnology Research Council.

Disclosure The experiments comply with the current laws of the country in which they were performed. The authors report no conflicts of interest.

References

1. Labauge P, Horzinski L, Ayrignac X, Blanc P, Vukusic S, Rodriguez D, Mauguiere F, Peter L, Goizet C, Bouhour F, Denier C, Confavreux C, Obadia M, Blanc F, de Sèze J, Fogli A, Boespflug-Tanguy O (2009) Natural history of adult-onset eIF2B-related disorders: a multi-centric survey of 16 cases. Brain 132:2161–2169
2. Li W, Wang X, van der Knaap MS, Proud CG (2004) Mutations linked to leukoencephalopathy with vanishing white matter impair the function of the eukaryotic initiation factor 2B complex in diverse ways. Mol Cell Biol 24:3295–3306

ARTHRITIS & RHEUMATISM
Vol. 64, No. 1, January 2012, pp 162–172
DOI 10.1002/art.33335

Overexpression of T-bet Gene Regulates Murine Autoimmune Arthritis

Yuya Kondo,[1] Mana Iizuka,[1] Ei Wakamatsu,[2] Zhaojin Yao,[1] Masahiro Tahara,[1] Hiroto Tsuboi,[1] Makoto Sugihara,[1] Taichi Hayashi,[1] Keigyou Yoh,[1] Satoru Takahashi,[1] Isao Matsumoto,[1] and Takayuki Sumida[1]

Objective. **To clarify the role of T-bet in the pathogenesis of collagen-induced arthritis (CIA).**

Methods. **T-bet–transgenic (Tg) mice under the control of the CD2 promoter were generated. CIA was induced in T-bet–Tg mice and wild-type C57BL/6 (B6) mice. Levels of type II collagen (CII)–reactive T-bet and retinoic acid receptor–related orphan nuclear receptor γt (RORγt) messenger RNA expression were analyzed by real-time polymerase chain reaction. Criss-cross experiments using CD4+ T cells from B6 and T-bet–Tg mice, as well as CD11c+ splenic dendritic cells (DCs) from B6 and T-bet–Tg mice with CII were performed, and interleukin-17 (IL-17) and interferon-γ (IFNγ) in the supernatants were measured by enzyme-linked immunosorbent assay. CD4+ T cells from B6, T-bet–Tg, or T-bet–Tg/IFNγ$^{-/-}$ mice were cultured for Th17 cell differentiation, then the proportions of cells producing IFNγ and IL-17 were analyzed by fluorescence-activated cell sorting.**

Results. **Unlike the B6 mice, the T-bet–Tg mice did not develop CIA. T-bet–Tg mice showed overexpression of *Tbx21* and down-regulation of *Rorc* in CII-reactive T cells. Criss-cross experiments with CD4+ T cells and splenic DCs showed a significant reduction in IL-17 production by CII-reactive CD4+ T cells in T-bet–Tg mice, even upon coculture with DCs from B6 mice, indicating dysfunction of IL-17–producing CD4+ T cells. Inhibition of Th17 cell differentiation under an in vitro condition favoring Th17 cell differentiation was observed in both T-bet–Tg mice and T-bet–Tg/IFNγ$^{-/-}$ mice.**

Conclusion. **Overexpression of T-bet in T cells suppressed the development of autoimmune arthritis. The regulatory mechanism of arthritis might involve dysfunction of CII-reactive Th17 cell differentiation by overexpression of T-bet via IFNγ-independent pathways.**

Rheumatoid arthritis (RA) is a chronic inflammatory disorder characterized by autoimmunity, infiltration of the joint synovium by activated inflammatory cells, and progressive destruction of cartilage and bone. Although the exact cause of RA is not clear, T cells seem to play a crucial role in the initiation and perpetuation of the chronic inflammation in RA.

The Th1 cell subset has long been considered to play a predominant role in inflammatory arthritis, because T cell clones from RA synovium were found to produce large amounts of interferon-γ (IFNγ) (1). Recently, interleukin-17 (IL-17)–producing Th17 cells have been identified, and this newly discovered T cell population appears to play a critical role in the development of various forms of autoimmune arthritis in experimental animals, such as those with glucose-6-phosphate isomerase–induced arthritis (2) and collagen-induced arthritis (CIA) (3). Conversely, IFNγ has antiinflammatory effects on the development of experimental arthritis (4,5). IL-17 is spontaneously produced by RA synovium (6), and the percentage of IL-17–positive CD4+ T cells

Supported in part by the Japanese Ministry of Science and Culture and by the Japanese Ministry of Health, Labor, and Welfare.

[1]Yuya Kondo, MD, Mana Iizuka, MSc, Zhaojin Yao, MSc, Masahiro Tahara, BSc, Hiroto Tsuboi, MD, PhD, Makoto Sugihara, MD, PhD, Taichi Hayashi, MD, PhD, Keigyou Yoh, MD, PhD, Satoru Takahashi, MD, PhD, Isao Matsumoto, MD, PhD, Takayuki Sumida, MD, PhD: Graduate School of Comprehensive Human Sciences, University of Tsukuba, Tsukuba City, Ibaraki, Japan; [2]Ei Wakamatsu, PhD: Graduate School of Comprehensive Human Sciences, University of Tsukuba, Tsukuba City, Ibaraki, Japan, and Harvard Medical School, Boston, Massachusetts.

Address correspondence to Takayuki Sumida, MD, PhD, Division of Clinical Immunology, Doctoral Programs in Clinical Sciences, Graduate School of Comprehensive Human Science, University of Tsukuba, 1-1-1 Tennodai, Tsukuba City, Ibaraki 305-8575, Japan. E-mail: tsumida@md.tsukuba.ac.jp.

Submitted for publication January 4, 2011; accepted in revised form September 1, 2011.

was increased in the peripheral blood mononuclear cells of patients with RA compared with healthy control subjects (7). It is therefore necessary to determine if autoimmune arthritis is a Th1- or a Th17-associated disorder.

The lineage commitment of each Th cell subset from naive CD4+ T cells is dependent on the expression of specific transcription factors induced under the particular cytokine environment. Differentiation of Th1 cells is dependent on the expression of the transcription factor T-bet, which is induced by IFNγ/STAT-1 signaling pathways and directly activates the production of IFNγ (8,9). Similarly, Th17 cell differentiation in mice is dependent on the transcription factor retinoic acid receptor–related orphan nuclear receptor γt (RORγt) induced by transforming growth factor β (TGFβ) and IL-6 (10). Previous studies showed that these transcription factors negatively regulate the differentiation of other T cell subsets by direct co-interaction and/or indirect effects of cytokines produced from each T cell subset (11,12). How the predominant differentiation of CD4+ T cells affects the development of autoimmune arthritis remains unclear, however.

In the present study, CIA was induced in C57BL/6 (B6) mice and T-bet–transgenic (Tg) mice under the control of the CD2 promoter. The results showed that CIA was significantly suppressed in T-bet–Tg mice as compared with B6 mice. IL-17 production was not detected in type II collagen (CII)–reactive T cells from T-bet–Tg mice, and a significant reduction in IL-17 production by CII-reactive CD4+ T cells from T-bet–Tg mice was observed even when they were cocultured with splenic dendritic cells (DCs) from B6 mice. IFNγ production was also reduced in T-bet–Tg mice as compared with B6 mice, and levels of IFNγ in CII-reactive CD4+ T cells from T-bet–Tg mice were not different from those in B6 mice. Inhibition of Th17 cell differentiation and predominant differentiation of Th1 cells under an in vitro condition favoring Th17 cell differentiation was observed in T-bet–Tg mice, and surprisingly, this inhibition was also observed in T-bet–Tg/IFNγ$^{-/-}$ mice. These results indicate suppression of Th17 cell differentiation by overexpression of T-bet, but not IFNγ. Our findings support the notion that the suppression of autoimmune arthritis in T-bet–Tg mice might be due to the direct inhibition of Th17 cell differentiation by T-bet overexpression in T cells.

MATERIALS AND METHODS

Mice. CD2 T-bet–Tg mice (12) were prepared by backcrossing mice on a C57BL/6 background. IFNγ$^{-/-}$ mice were obtained from The Jackson Laboratory. Littermates of T-bet–Tg mice were used as controls in all experiments. All mice were maintained under specific pathogen–free conditions, and the experiments were conducted in accordance with the institutional ethics guidelines.

Induction of CIA and assessment of arthritis. Native chicken CII (Sigma-Aldrich) was dissolved in 0.01*M* acetic acid and emulsified in Freund's complete adjuvant (CFA). CFA was prepared by mixing 5 mg of heat-killed *Mycobacterium tuberculosis* H37Ra (Difco) and 1 ml of Freund's incomplete adjuvant (Sigma-Aldrich). Mice ages 8–10 weeks were injected intradermally at the base of the tail with 200 μg of CII in CFA on days 0 and 21. Arthritis was evaluated visually, and changes in each paw were scored on a scale of 0–3, where 0 = normal, 1 = slight swelling and/or erythema, 2 = pronounced swelling, and 3 = ankylosis. The scores in the 4 limbs were then summed (maximum score 12).

Histopathologic scoring. For histologic assessment, mice were killed on day 42 after the first immunization, and both rear limbs were removed. After fixation and decalcification, joint sections were cut and stained with hematoxylin and eosin. Histologic features of arthritis were quantified by 2 independent observers (YK and IM) who were blinded with regard to the study group, and a histologic score was assigned to each joint based on the degree of inflammation and erosion, as described previously (13). The severity of inflammation was scored on a scale of 0–5, where 0 = normal, 1 = minimal inflammatory infiltration, 2 = mild infiltration with no soft tissue edema or synovial lining cell hyperplasia, 3 = moderate infiltration with surrounding soft tissue edema and some synovial lining cell hyperplasia, 4 = marked infiltration, edema, and synovial lining cell hyperplasia, and 5 = severe infiltration with extended soft tissue edema and marked synovial lining cell hyperplasia. The severity of bone erosion was also scored on a scale of 0–5, where 0 = none, 1 = minimal, 2 = mild, 3 = moderate, 4 = marked, and 5 = severe erosion with full-thickness defects in the cortical bone.

Analysis of cytokine profiles and cytokine and transcriptional factor gene expression. Inguinal and popliteal lymph nodes were harvested from each mouse on day 10 after the first immunization with CII. Single-cell suspensions were prepared, and lymph node cells (2×10^5/well on a 96-well round-bottomed plate) were cultured for 72 hours in RPMI 1640 medium (Sigma-Aldrich) containing 10% fetal bovine serum, 100 units/ml of penicillin, 100 μg/ml of streptomycin, and 50 μ*M* 2-mercaptoethanol in the presence of 100 μg/ml of denatured chicken CII. The supernatants were analyzed for IFNγ, IL-4, IL-10, and IL-17 by enzyme-linked immunosorbent assay (ELISA) using specific Quantikine ELISA kits (R&D Systems).

Lymphocytes harvested on day 10 after immunization were used to obtain complementary DNA (cDNA) by reverse transcription, using a commercially available kit. A TaqMan Assay-on-Demand gene expression product was used for real-time polymerase chain reaction (PCR; Applied Biosystems). The expression levels of *Ifng*, *Il17a*, *Tbx21*, *Rorc*, *Il12a*, and *Il23a* were normalized relative to the expression of *gapdh*. Analyses were performed with an ABI Prism 7500 apparatus (Applied Biosystems).

Criss-cross coculture with CD4+ T cells and CD11c+ splenic dendritic cells. Ten days after the first CII immunization, CD4+ cells in draining lymph nodes were isolated by

positive selection, using a magnetic-activated cell sorter (MACS) system with anti-CD4 monoclonal antibody (mAb; Miltenyi Biotec). After treatment with mitomycin C, CD11c+ cells were isolated from the spleen by positive selection, using a MACS system with anti-CD11c mAb (Miltenyi Biotec). Criss-cross coculture for 72 hours was performed with 1×10^5 CD4+ cells and 2×10^4 CD11c+ cells in 100 μg/ml of denatured CII-containing medium. Cytokine production and transcription factor expression were then analyzed.

Measurement of collagen-specific immunoglobulin titers. Serum was collected from the mice on day 56 after the first immunization. A total of 10 μg/ml of CII in phosphate buffered saline (PBS) was coated overnight at 4°C onto 96-well plates (Nunc MaxiSorp; Nalge Nunc). After washes with washing buffer (0.05% Tween 20 in PBS), the blocking solution, including 1% bovine serum albumin in PBS, was applied for 1 hour. After washing, 100 μl of diluted serum was added, and the plates were incubated for 1 hour at room temperature. After further washing, horseradish peroxidase–conjugated anti-mouse IgG, IgG1, IgG2a, or IgG2b (1:5,000 dilution) in blocking solution was added, and the plates were incubated for 1 hour at room temperature. After washing, tetramethylbenzidine was added, and the optical density was read at 450 nm using a microplate reader.

Purification of CD4+ cells and in vitro T cell cultures. CD4+ cells (1×10^6/well) were cultured in medium with 1 μg/ml of soluble anti-CD3ε mAb (eBioscience), 1 μg/ml of soluble anti-CD28 mAb (BioLegend), 10 μg/ml of anti-IFNγ mAb (BioLegend), and 10 μg/ml of anti–IL-4 mAb (BioLegend) for a neutral condition. For Th17 cell differentiation, CD4+ cells (1×10^6/well) were cultured in medium with 1 μg/ml of soluble anti-CD3ε mAb, 1 μg/ml of soluble anti-CD28 mAb, 3 ng/ml of human TGFβ (R&D Systems), 20 ng/ml of mouse IL-6 (eBioscience), 10 μg/ml of anti-IFNγ mAb, and 10 μg/ml of anti–IL-4 mAb. On day 4, cells were restimulated for 4 hours with 50 ng/ml of phorbol myristate acetate and 500 ng/ml of ionomycin and used in the experiments.

Surface and intracellular staining and fluorescence-activated cell sorter (FACS) analysis. GolgiStop (BD PharMingen) was added during the last 6 hours of each culture. Cells were stained extracellularly, fixed, and permeabilized with Cytofix/Cytoperm solution (BD PharMingen). Then, intracellular cytokine staining was performed according to the manufacturer's protocol, using fluorescein isothiocyanate (FITC)–conjugated anti-IFNγ (BD PharMingen) and phycoerythrin (PE)–conjugated anti–IL-17 (BD PharMingen) or FITC-conjugated anti–IL-17 (BioLegend). A Treg cell staining kit (eBioscience) was used to stain T-bet, RORγt, and FoxP3 in cultured cells according to the manufacturer's protocol, using PE-conjugated anti–T-bet (eBioscience), allophycocyanin-conjugated anti-RORγt (eBioscience), and PE-conjugated anti-FoxP3 (eBioscience). Samples were analyzed with a FACSCalibur flow cytometer (Becton Dickinson), and data were analyzed with FlowJo software (Tree Star).

Statistical analysis. Data are expressed as the mean ± SEM or the mean ± SD. Differences between groups were examined for statistical significance using Student's *t*-test. *P* values less than 0.05 were considered significant.

RESULTS

Construction of the T-bet transgene and tissue distribution of transcription factors and cytokine production in naive mice. To generate transgenic mouse lines that express high levels of T-bet specifically in T cells, mouse T-bet cDNA was inserted into a VA vector containing a human CD2 transgene cassette (14). To confirm the expression of the transgene, reverse transcription–PCR (RT-PCR) was performed to monitor the expression of *Tbx21* (coding for T-bet) in organs from the T-bet–Tg mice. *Tbx21* messenger RNA (mRNA) expression was detected in the lymphatic system and in nonlymphatic organs in T-bet–Tg mice, and the expression levels were higher than those in B6 mice (data available upon request from the author). Analysis by semiquantitative RT-PCR and quantitative PCR (data not shown) revealed that the expression levels of other transcription factors (*Gata3*, *Rorc*, and *Foxp3*) in T-bet–Tg mice were not different from those in B6 mice. As previously reported by Ishizaki et al (14), high production of IFNγ was observed even when CD4+ T cells isolated from the spleen of T-bet–Tg mice were cultured under neutral conditions (data available upon request from the author).

Failure to induce CIA and low CII-specific IgG production in T-bet–Tg mice. To assess whether T cell–specific T-bet expression affects the development of arthritis, we induced CIA in T-bet–Tg mice and in wild-type B6 mice. The incidence and severity of arthritis in T-bet–Tg mice were markedly suppressed compared with those in B6 mice (Figure 1A). Surprisingly, the majority of T-bet–Tg mice were essentially free of arthritis, and even when arthritis was present, it was of the mild type. Consistent with these findings, histologic analyses of the joints obtained from each mouse 42 days after immunization revealed that joint inflammation and destruction were significantly suppressed in T-bet–Tg mice compared with B6 mice (Figures 1B and C). These results indicated that enforced expression of T-bet in T cells suppressed the development of CIA.

Because the levels of CII-specific IgG correlate well with the development of arthritis (15), we examined CII-specific IgG production in T-bet–Tg mice. CII-specific IgG, IgG1, IgG2a, and IgG2b levels were significantly lower in T-bet–Tg mice than in B6 mice, as determined by ELISA (Figure 1D). Thus, enforced expression of T-bet in T cells suppresses the development of CIA and CII-specific IgG production.

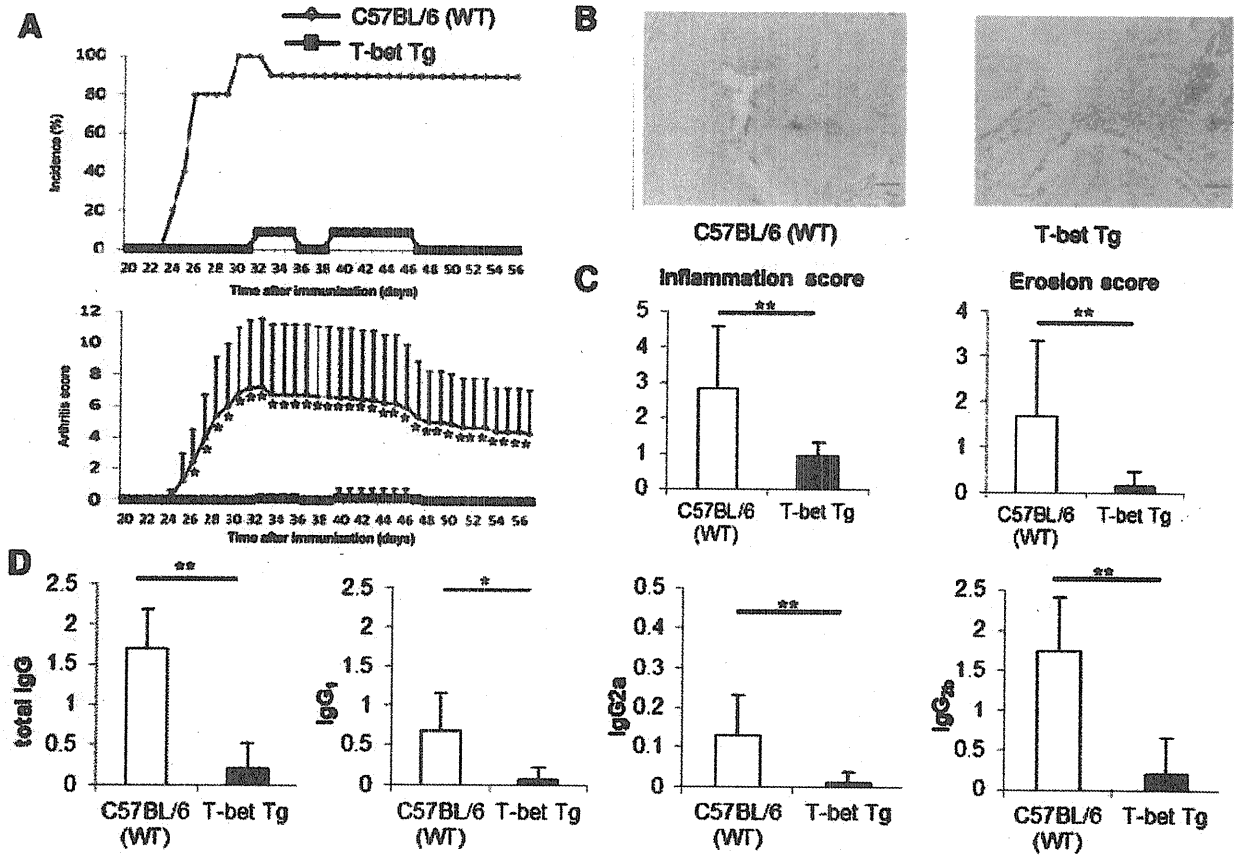

Figure 1. Significant suppression of collagen-induced arthritis (CIA) and type II collagen (CII)–specific IgG production in T-bet–transgenic (Tg) mice. On days 0 and 21, mice were immunized intradermally at several sites at the base of the tail with chicken CII emulsified with Freund's complete adjuvant. **A,** Incidence and severity of CIA. The arthritis score was determined as described in Materials and Methods. Data were obtained from 2 independent experiments involving 10 C57BL/6 (wild-type [WT]) mice and 11 T-bet–Tg mice. **B,** Hematoxylin and eosin–stained sections of the hind paws of mice obtained 6 weeks after the first immunization. Original magnification × 40. **C,** Inflammation and bone erosion scores in 7 C57BL/6 mice and 5 T-bet–Tg mice 6 weeks after the first immunization. Scores were determined as described in Materials and Methods. **D,** Serum levels of CII-specific IgG, IgG1, IgG2a, and IgG2b levels in 10 C57BL/6 mice and 11 T-bet–Tg mice 8 weeks after the first immunization, as measured by enzyme-linked immunosorbent assay. Values in A, C, and D are the mean ± SD. * = $P < 0.05$; ** = $P < 0.01$ by Student's *t*-test.

Suppression of CII-reactive IL-17 production and IL-17 mRNA expression in T-bet–Tg mice. Because enforced T-bet expression in T cells suppressed the development CIA, we examined antigen-specific cytokine production and transcription factor expression in mice with CIA. CD4+ T cells harvested from draining lymph nodes were stimulated with CII in vitro, and then various cytokine levels in the supernatants were measured by ELISA. IL-17 production by CII-reactive T cells was significantly reduced in T-bet–Tg mice as compared with B6 mice (Figure 2A). IFNγ production by CII-reactive T cells also tended to be decreased in T-bet–Tg mice.

We analyzed CII-reactive cytokine and transcription factor mRNA expression levels by real-time PCR (Figure 2B). Similar to the ELISA results, *Il17a* expression tended to be lower in T-bet–Tg mice than in B6 mice. No difference in *Ifng* expression was observed between B6 and T-bet–Tg mice (Figure 2B). *Tbx21* expression tended to be higher in T-bet–Tg mice, whereas *Rorc* expression was lower in T-bet–Tg mice than in B6 mice ($P < 0.05$). The level of expression of *Il12a* (coding for IL-12p35) was also higher in T-bet–Tg mice than in B6 mice ($P < 0.05$). However, there was no difference in the expression levels of *Il23a* (coding for IL-23p19) between B6 mice and T-bet–Tg mice. These

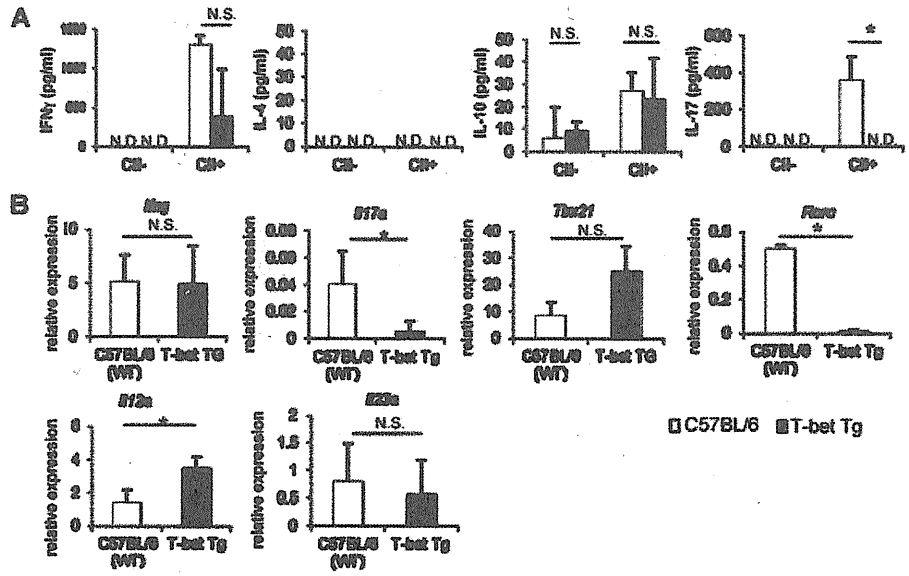

Figure 2. No production of interleukin-17 (IL-17) and low production of interferon-γ (IFNγ) in type II collagen (CII)–reactive CD4+ T cells. **A**, Ten days after the first CII immunization, lymphocytes derived from the draining lymph nodes of C57BL/6 (wild-type [WT]) mice and T-bet–transgenic (Tg) mice were cultured for 72 hours in the presence or absence of 100 μg/ml of denatured CII. Levels of IL-17, IFNγ, IL-4, and IL-10 in the supernatants were measured by enzyme-linked immunosorbent assay. **B**, After culture of lymphocytes with CII, cDNA was obtained, and levels of *Ifng*, *Il17a*, *Tbx21*, *Rorc*, *Il12a*, and *Il23a* expression were analyzed by real-time polymerase chain reaction. Values are the mean ± SD of 3 mice. * = $P < 0.05$ by Student's *t*-test. ND = not detected; NS = not significant.

results suggest that overexpression of T-bet on CD4+ T cells suppressed the expression of RORγt and IL-17.

No reduction of RORγt expression on CII-reactive CD4+ T cells in T-bet–Tg mice. CD4+ T cells from T-bet–Tg and B6 mice were cultured in vitro with CII, and analyses of T-bet and RORγt expression on CD4+ T cells were carried out by the intracellular staining method. T-bet expression on CII-reactive CD4+ T cells was significantly higher in T-bet–Tg mice than in B6 mice (Figure 3A). Surprisingly, the majority of T-bet+ CII-reactive T cells expressed RORγt in both the B6 mice and the T-bet–Tg mice (Figure 3A). Although there was no significant difference in the mean fluorescence intensity of RORγt between B6 mice and T-bet–Tg mice, the number of RORγt+ cells tended to be lower in T-bet–Tg mice (data available upon request from the author).

Moreover, in the case of CD4+ T cells examined under conditions favoring Th17 differentiation, RORγt expression on CD4+ T cells from T-bet–Tg mice was lower than that on cells from B6 mice (Figure 3B). Interestingly, most of the RORγt+ cells also expressed T-bet in the T-bet–Tg mice, and the proportion of IL-17–producing RORγt+ CD4+ T cells was lower in the T-bet–Tg mice than in the B6 mice. These findings support the notion that overexpression of T-bet not only suppresses RORγt expression on CD4+ T cells but also inhibits the production of IL-17 from RORγt+ T cells.

To investigate whether the suppression of arthritis and low antigen-specific cytokine production observed in T-bet–Tg mice was related to Treg cells, the next experiment analyzed FoxP3 expression on CD4+ T cells harvested from draining lymph nodes 10 days after immunization. There was no significant difference in the percentage of FoxP3+ cells among the CD4+ T cells between B6 mice and T-bet–Tg mice (data available upon request from the author). Thus, Treg cells do not seem to be involved in the suppression of CIA in T-bet–Tg mice.

Decreased numbers of T cells in the lymph nodes, spleen, and thymus of T-bet–Tg mice. To evaluate the low cytokine response and the low population of CII-reactive RORγt+CD4+ T cells in T-bet–Tg mice with CIA, we analyzed the lymphocyte subsets in the draining lymph nodes and spleen after immunization. The percentage and absolute number of CD3+ T cells were lower in both the draining lymph nodes and the

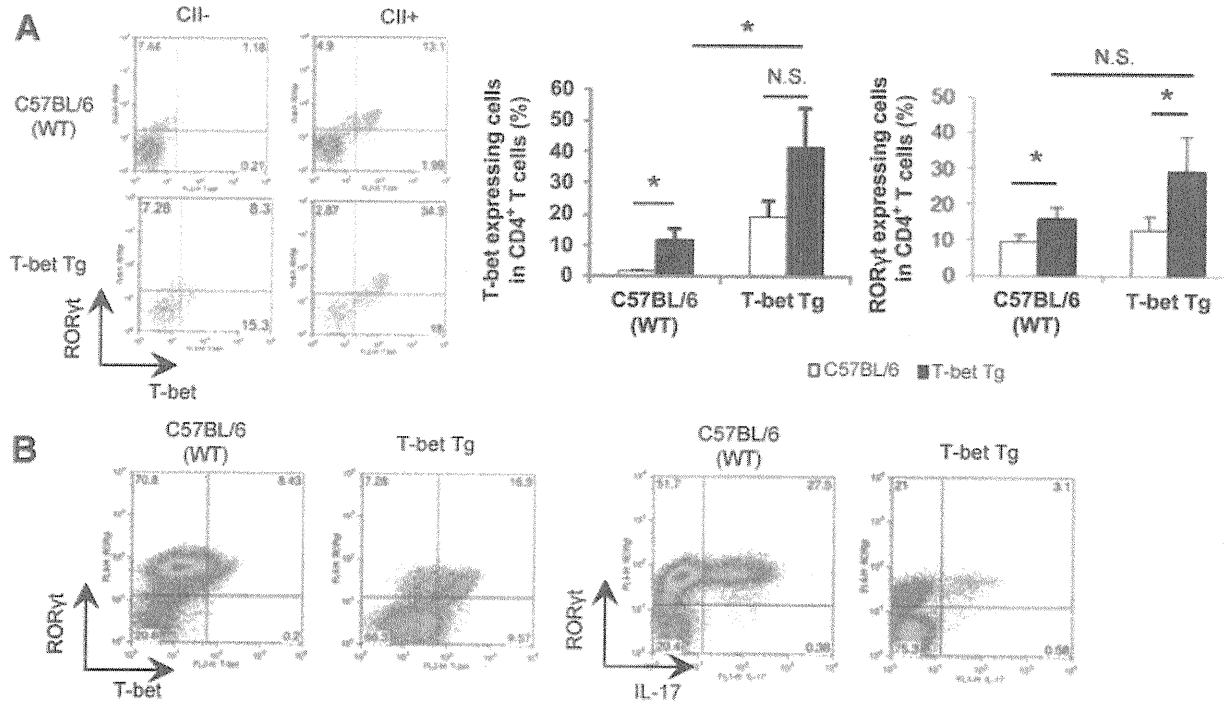

Figure 3. Suppression of Th17 cell differentiation by enforced expression of T-bet in T cells despite expression of retinoic acid receptor–related orphan nuclear receptor γt (RORγt). **A**, Ten days after the first type II collagen (CII) immunization, lymphocytes derived from the draining lymph nodes of C57BL/6 (wild-type [WT]) and T-bet–transgenic (Tg) mice were cultured for 72 hours in the presence or absence of 100 μg/ml of denatured CII. Levels of T-bet and RORγt expression on CD4+ T cells were analyzed by intracellular staining. Numbers in each compartment of the histograms are the percentage of transcription factor–expressing cells gated on CD4+ T cells. Values in the bar graphs are the mean ± SD of 3 mice per group. * = $P < 0.05$ by Student's *t*-test. NS = not significant. **B**, CD4+ T cells were isolated from the spleen of C57BL/6 and T-bet–Tg mice by magnetic-activated cell sorting and were then cultured for 96 hours with soluble anti-CD3 antibody, soluble anti-CD28 antibody, interleukin-6 (IL-6), and transforming growth factor β. Cytokine production and transcription factor expression on CD4+ T cells were analyzed by intracellular staining. Representative histograms from flow cytometric analysis of T-bet and RORγt expression with IL-17 production are shown. Numbers in each compartment are the percentage of positive cells gated on CD4+ T cells.

spleen of T-bet–Tg mice as compared with B6 mice (Figures 4A and B). The absolute number of CD4+ and CD8+ T cells also tended to be lower in T-bet–Tg mice (Figure 4B). Moreover, analysis of the thymus showed a significantly low number of total thymocytes in T-bet–Tg mice and the presence of an abnormal proportion of T precursor cells, such as a low number of double-positive T cells and CD4 single-positive T cells in T-bet–Tg mice (Figure 4C). These results suggest abnormal T cell development in the thymus of T-bet–Tg mice.

Inhibition of IL-17 production by CII-reactive CD4+ T cells in T-bet–Tg mice. To clarify whether T-bet overexpression on CD4+ T cells directly affects cytokine production, we performed criss-cross experiments using CD4+ T cells from B6 and T-bet–Tg mice, as well as DCs from B6 and T-bet–Tg mice in CII–containing medium, and measured IL-17 and IFNγ levels in the supernatants by ELISA. IL-17 production was detected in CII-reactive CD4+ T cells from B6 mice and in DCs from T-bet–Tg mice. Interestingly, IL-17 production was significantly reduced, even when CD4+ T cells from T-bet–Tg mice were cocultured with DCs from B6 mice (Figure 5A). These observations suggest that T-bet overexpression on CD4+ T cells is responsible for the inhibition of CII-reactive IL-17 production. No difference in IFNγ production was noted among the experimental conditions (Figure 5A), suggesting that reduced IFNγ production by CII-reactive CD4+ T cells from T-bet–Tg mice (Figure 2) was probably related to the reduced numbers of CD4+ T cells in draining lymph nodes. Moreover, intracellular staining revealed that RORγt expression was suppressed and T-bet expression was increased, even when CD4+ T cells from T-bet–Tg

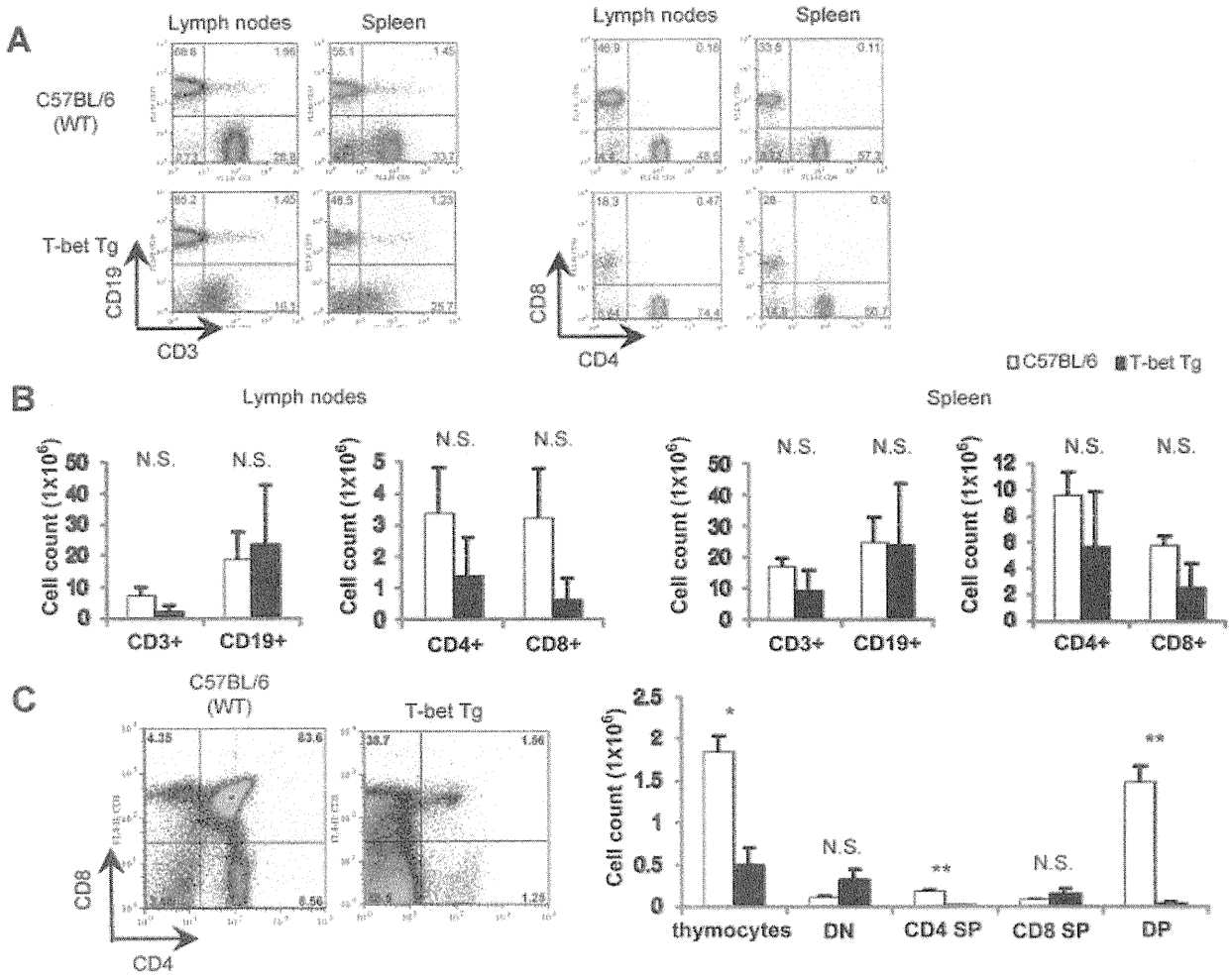

Figure 4. Decreased number of CD3+ T cells in spleen and lymph nodes and abnormal development of T precursor cells in the thymus in T-bet–transgenic (Tg) mice. **A**, Ten days after first immunization, the proportion of lymphocytes in draining lymph nodes and spleen were analyzed by fluorescence-activated cell sorting (FACS), and the absolute numbers of cells were calculated. Numbers in each compartment are the percentage of the parent population. **B**, The absolute numbers of CD3+, CD19+, CD4+, and CD8+ T cells in the lymph nodes and spleen of C57BL/6 (wild-type [WT]) and T-bet–Tg mice were determined. Values are the mean ± SD of 3 mice per group. NS = not significant. **C**, The proportion of T precursor cells in the thymus of nonimmunized mice was analyzed by FACS, and the absolute numbers of thymocytes, double-negative (DN) T cells, CD4 and CD8 single-positive (SP) T cells, and double-positive (DP) T cells were determined. Values in the bar graphs are the mean ± SD of 3 mice per group. * = $P < 0.05$; ** = $P < 0.01$ by Student's *t*-test.

mice were cocultured with DCs from B6 mice (Figure 5B). These results indicate that T-bet overexpression on CD4+ T cells suppressed CII-reactive IL-17 production by inhibition of the expression of RORγt.

Overexpression of T-bet directly suppresses Th17 cell differentiation via IFNγ-independent mechanisms. To clarify whether IFNγ production influences Th17 cell differentiation, we generated T-bet–Tg/IFNγ$^{-/-}$ mice. CD4+ T cells were isolated from the spleen of T-bet–Tg, T-bet–Tg/IFNγ$^{-/-}$, and B6 mice and were then cultured for Th17 cell differentiation. FACS analysis demonstrated that the proportion of IL-17–producing CD4+ T cells was lower in T-bet–Tg mice than in B6 mice, whereas the proportion of IFNγ-producing CD4+ T cells was higher in T-bet–Tg mice. Similarly, the proportion of IL-17–producing CD4+ T cells was also lower in T-bet–Tg/IFNγ$^{-/-}$ mice, although no IFNγ-producing CD4+ T cells were detected in

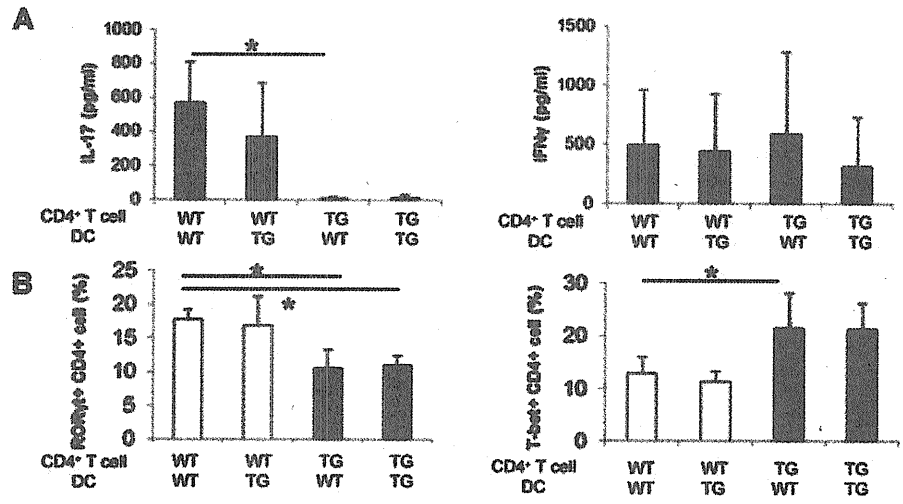

Figure 5. Impaired antigen-specific Th17 cell responses in T-bet–transgenic (Tg) mice with collagen-induced arthritis (CIA). Ten days after the first type II collagen (CII) immunization, CD4+ cells were isolated from draining lymph nodes of C57BL/6 (wild-type [WT]) mice and T-bet–Tg (TG) mice by positive selection using magnetic-activated cell sorting (MACS) with anti-CD4 monoclonal antibody (mAb). After treatment with mitomycin C, CD11c+ cells were isolated from the spleen by positive selection using a MACS system with anti-CD11c mAb. Criss-cross coculture for 72 hours was performed with 1×10^5 CD4+ cells and 2×10^4 CD11c+ cells in 100 μg/ml of denatured CII–containing medium. **A**, Levels of interleukin-17 (IL-17) and interferon-γ (IFNγ) in culture supernatants were measured by enzyme-linked immunosorbent assay. **B**, Expression of retinoic acid receptor–related orphan nuclear receptor γt (RORγt) and T-bet expression on CD4+ T cells were analyzed by intracellular staining. Representative data from flow cytometric analysis of the percentage of RORγt+ or T-bet+ cells in the CD4+ T cell subset are shown. Values are the mean ± SD of 3 mice per group. * = $P < 0.05$ by Student's *t*-test. DC = dendritic cells.

T-bet–Tg/IFN$\gamma^{-/-}$ mice (Figure 6). These results strongly support the view that inhibition of Th17 cell differentiation in T-bet–Tg mice cannot be due to overproduction of IFNγ, indicating that overexpression of T-bet directly suppresses Th17 cell differentiation in T-bet–Tg mice.

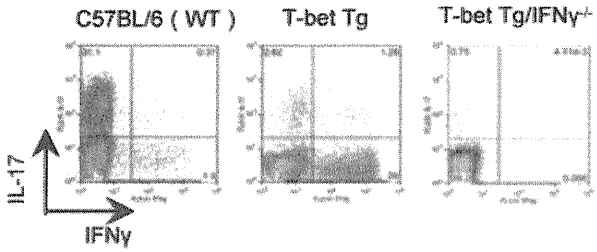

Figure 6. Suppressed expression of interleukin-17 (IL-17) by T-bet overexpression independently of interferon-γ (IFNγ) in T-bet–transgenic (Tg) mice. CD4+ T cells were isolated from the spleen of C57BL/6 (wild-type [WT]), T-bet–Tg, and T-bet–Tg/IFN$\gamma^{-/-}$ mice by magnetic-activated cell sorting and then cultured for 96 hours with soluble anti-CD3 monoclonal antibody (mAb), soluble anti-CD28 mAb, IL-6, and transforming growth factor β. IFNγ and IL-17 production by CD4+ cells was analyzed by intracellular cytokine staining. Numbers in each compartment are the percentage of cells secreting cytokines.

DISCUSSION

Recent studies showed that IL-17 plays a crucial role in the development of CIA (3) and other types of experimental arthritis (2). In contrast, it has been reported that IFNγ can suppress IL-17 production in vitro (16) and has antiinflammatory effects on the development of experimental arthritis (4,5). T-bet is a transcription factor known to induce the differentiation of naive CD4+ T cells to Th1 cells (8). Although the absence of T-bet can result in severe IL-17–mediated experimental autoimmune myocarditis via dysregulation of IFNγ (17), several studies have shown that T-bet is essential for the development of several models of autoimmunity, such as experimental autoimmune encephalitis (18,19), colitis (20), and diabetes mellitus (21). Nevertheless, the effect of T-bet expression on Th17 cell differentiation and function during arthritis remains unclear.

T-bet–Tg mice overexpress T-bet and mainly produce IFNγ in their T cells (14). Previous studies in T-bet–Tg mice suggested that overexpression of T-bet and a predominant Th1 response affect the pathogenesis of various diseases (14,22,23). To examine whether T-bet overexpression on T cells affects the regulation of